# Fully Implicit Form of Differential Quadrature Method for Multi-Species Solute Transport in Porous Media

Amin GHAREHBAGHI[1]

## ABSTRACT

Solute transport problems, including sequential multi-species transport phenomena, frequently occur in soil systems. The goal of this paper is to present a novel one-dimensional numerical model with a fully implicit form of differential quadrature method for solving multi-species solute transport equations. The analytical results of three multi-species solute dispersion problems with three- and four-chain members are used to analyse the developed model. Simultaneously, the outcomes of the developed model are compared with the performance of the fully implicit fourth-order finite difference method. Finally, the accuracy of the established model is discussed and evaluated. According to the numerical experiments, the derived model is very useful and widely applicable.

**Keywords**: Multi-species, solute transport, porous media, Fully Implicit Differential Quadrature Method, Fully Implicit Fourth-Order Finite Difference Method.

## 1. INTRODUCTION

To manage groundwater and surface water resources, the estimation of the solute and contaminant transport phenomena is significant. Due to the impact of this issue in human life, numerous experimental studies carried out in this field, and various numerical and analytical models have been developed by researchers. Nevertheless, most of the analytical and numerical models developed only for describing single-member transport of various contaminants (Kumar et al., 2010; Savovic and Djordjevich 2012; Singh et al., 2012; Gharehbaghi 2016 & 2017; Ciftci, 2017; Das et al., 2018; among many). But, the transport processes of some dangerous contaminants, e.g., pesticides and their degradation products, generally include a more complicated series of first-order or pseudo-first-order decay. Accordingly, single-member transport models cannot calculate the process of degradable contaminants transformation from the parent species to the daughter species. In other respects, mostly analytical solutions have specific and restricted enforcements. Therefore, one-, two-, or three-dimensional (1D, 2D, 3D) analytical solutions in this field (e.g., Van Genuchten 1985, Sun 1999 et al., Chaudhary and Singh 2020) have their limitations. To the

1 Hasan Kalyoncu University, Civil Engineering Department, Gaziantep, Turkey
  amin.gharehbaghi@hku.edu.tr - https://orcid.org/0000-0002-2898-3681

best of author's knowledge, in numerical modeling, most scientists prefer to employ one of the conventional methods such as finite difference method (FDM), finite element method (FEM), or finite volume method (FVM). (Gharehbaghi et al., 2017). However, new numerical techniques such as the differential quadrature method (DQM), have many advantages over the traditional methods. One of the advantages of DQM is that it could calculate more accurate outcomes by using a small number of nodes in space and time. Moreover, DQM normally prevents confusion and linearization to obtain more accurate solutions of given nonlinear equations. As a global numerical method, DQM employs more points in the model domain to estimate the functional value of a certain point. Therefore, it provides rapidly converging and more reliable results than FEM or FDM, particularly in nonlinear problems (Chen and Zhong, 1997). The traditional numerical techniques are developed on relatively complicated mathematical derivations and require sophisticated mathematical calculations; more struggle in the discretization process. "The DQM is capable of producing solutions at high accuracy, with fewer grid points, comparatively little computational effort and less storage requirements" (Ciftci 2017). According to the study carried out by Gharehbaghi (2016), the fully implicit form of the solution with DQM (IDQM) obtained more accurate outcomes than the explicit form. Consequently, in this paper, the author employed IDQM. The summaries of several studies, related to this paper in 1D form, are presented as follows:

Konikow and Bredehoeft (1978) developed a 2D numerical model, called MOC, by employing an implicit form of FDM to determine the average linear flow velocities. Subsequently, these calculated values are employed to solve the transport equation by applying the method of characteristics. Later, Essaid and Bekins (1997) improved the MOC and named it BIOMOC. They announced that the BIOMOC model simulated the 2D transport and biotransformation of multiple reacting solutes. Massoudieh and Ginn (2007) presented an integrated unsaturated flow and colloid-facilitated contaminant transport model for multiple species with competitive sorption. They announced that the unsaturated flow part of the model and colloid-facilitated transport part of the model solved employing a semi-implicit FDM with Crank–Nicholson time weighing scheme, and fully coupled implicit FDM with dynamic blocking function $B$ evaluated explicitly from the previous time step, respectively. Chen-Charpentier et al., (2009) presented a numerical model for the flow, the transport of nutrients and contaminants, and the growth of two types of microorganisms in porous media to gain a better understanding of the interactions between two microbial species as part of a single biofilm capable of performing multiple functions (bioremediation, biofilm formation, etc.). They solved the coupled system of equations by using mixed-finite elements for the flow and a non-standard method for the transport equations. Natarajan and Kumar (2010) proposed an alternative approach to the decomposition method for solving multispecies transport in porous media coupled with first-order reactions. They developed the numerical solution based on the implicit FDM. Ramos et al., (2011) carried out several experimental studies and employed HYDRUS-1D software package based on the Galerkin-type linear finite element schemes to assess soil salinization and sodification risks. Torlapati (2013) established a multi-component reactive transport model to simulate the fate and transport of biochemical and geochemical reactive transport problems in 1D conditions. He employed explicit forms of backward difference FDM and total variation diminishing schemes and fully implicit approaches for solving the governing equations. Bagalkot and Kumar (2015) carried out a 1D numerical analysis on multispecies radionuclide transport in

a single-horizontal coupled fracture-matrix system by FDM. They considered Linear, Langmuir, and Freundlich adsorption isotherms and the results from each were compared. Sharma et al., (2016) by using constant, linear, and exponential dispersivity functions investigated the influence of distance-dependent dispersion on the multispecies solute transport process. They used implicit FDM and discretized the governing equations with upwind and central difference schemes. Engdahl and Aquino (2018) studied the possibility of backward-in-time simulations on nonlinear reactive transport systems in an operational sense. They simulated a steady-state flow field employing a second-order, cell-centered implicit FDM. Zhang et al., (2018) suggested a 1D model based on the Maxwell-Stefan diffusion theory and the MCL equation. Moreover, numerical simulation was carried out using the finite element software COMSOL Multiphysics. Pathania et al., (2020) suggested a numerical model based on the meshless element-free Galerkin method to predict the groundwater flow and multispecies reactive transport coupled with sequential decay reactions in unconfined aquifers. They compared the results of the developed model with FDM, FEM, and MODFLOW-RT3D.

The motive for this research is to provide a powerful and effective mathematical model based on the fully implicit form of the DQM for the first time for solving the multi-species solute transport phenomenon in 1D form with advection-dispersion equation (ADE). Unlike other researchers, who generally deal with the problem explicitly, in this research, I have considered the fully implicit form of the solution. In this paper, three analytical solutions are extracted from the studies of Bauer et al., (2001) and Pérez Guerrero et al., (2009) to assess the outcomes of the derived model. Likewise, the fully implicit fourth-order finite difference method (IFOFDM) is developed and employed to examine the performance of the enforced scheme in the established model.

## 2. PROBLEM FORMULATION

A series of chemical intermediates or radionuclides coupled with first-order decay processes form a decay chain. From the mathematical point of view, for reactive multi-species solute transport that is subject to linear equilibrium sorption and includes a sequential first-order decay chain, the governing equations are written as follows: (Bauer et al. 2001; Pérez Guerrero et al. 2009):

$$R_m \frac{\partial c_m}{\partial t} = D \frac{\partial^2 c_m}{\partial x^2} - v \frac{\partial c_m}{\partial x} - R_m \lambda_m c_m + R_{m-1} \lambda_{m-1} c_{m-1}; \; m = 1, \ldots, M; \; \lambda_0 = 0; \; 0 < x < \infty; t > 0; \tag{1}$$

where $c_m$, $R_m$, $D$, $v$, $\lambda_m$, $x$, and $t$ are the concentration of the $m^{th}$ member of the decay chain formed by $M$ species, the retardation coefficient for the $m^{th}$ species, the dispersion coefficient, the constant pore water velocity, the first-order decay constant for the $m^{th}$ species, the longitudinal axis, and time, respectively. To simplify in Eq. (1), instead of $R_m \lambda_m$, the symbol of $k_m$ is used.

## 3. NUMERICAL INVESTIGATION

As underlined earlier, in this paper, a fully implicit form of solution for two different numerical methods (i.e., IDQM and IFOFDM) is employed to solve the governing equations. The chief idea behind DQM is based on the Gauss Quadrature method. ''Extending Gauss quadrature to finding the derivatives of various orders of a differentiable function gives rise to differential quadrature" (Bellman and Casti, 1971). For the first time, Bellman introduced this method. Afterward, other researchers such as Shu (2000), Civalek (2004), Kaya (2010), Kaya and Arisoy (2011), Gharehbaghi (2016) tried to improve and apply this technique to the various fields of engineering. About this study, even though the suggested model has no restrictions on the number of multi-species since the analytical solutions applied were developed for a maximum of four species, solutions for four species are presented in this paper. In this step, the numerical solution of IDQM for the first member by substituting the value of $m$ as one in Eq. (1) (i.e., $m=1$) is given as follows:

$$R_1 \frac{\partial C_1}{\partial t} = D \frac{\partial^2 C_1}{\partial x^2} - v \frac{\partial C_1}{\partial x} - k_1 C_1 \quad 0 < x < \infty, \quad t > 0 \tag{2}$$

Based on the DQM, the first- and second-order derivatives for each node are arranged as follows:

$$\frac{\partial C_1}{\partial x} = \sum_{j=1}^{N} a_{ij} C_{1_j} = (a_{i1} C_{1_1} + a_{i2} C_{1_2} + a_{i3} C_{1_3} + \cdots + a_{iN} C_{1_N}) \tag{3}$$

$$\frac{\partial^2 C_1}{\partial x^2} = \sum_{j=1}^{N} b_{ij} C_{1_j} = (b_{i1} C_{1_1} + b_{i2} C_{1_2} + b_{i3} C_{1_3} + \cdots + b_{iN} C_{1_N}) \tag{4}$$

where $a_{ij}$ and $b_{ij}$ are the weighting coefficients of the first- and second-order derivatives, respectively. With respect to the notations of the DQM, Eq. (5) is rewritten as follows

$$R_1 \frac{\partial C_1}{\partial t} = D \sum_{j=1}^{N} b_{ij} C_{1_j} - v \sum_{j=1}^{N} a_{ij} C_{1_j} - k_1 C_1 \tag{5}$$

The values of weighting coefficients are calculated by the following relations (Zong and Zhang, 2009):

$$a_{ij} = \frac{1}{(x_j - x_i)} \bigcap_{\substack{k=1 \\ k \neq i,j}}^{N} \frac{x_i - x_k}{x_j - x_k} \quad i,j = 1,2, \dots, N; \ i \neq j \tag{6}$$

$$a_{ii} = -\sum_{\substack{j=1 \\ j \neq i}}^{N} a_{ij} \quad i,j = 1,2, \dots, N \tag{7}$$

$$b_{ij} = 2 \left[ a_{ij}. a_{ii} - \frac{a_{ij}}{(x_j - x_i)} \right] \quad i,j = 1,2, \dots, N; \ i \neq j \tag{8}$$

$$b_{ii} = -\sum_{\substack{j=1 \\ j \neq i}}^{N} b_{ij} \quad i,j = 1,2, \dots, N \tag{9}$$

where $\cap$ denotes the product sign. To calculate the node distributions several approaches were proposed by the experts. ''It can be selected with equal intervals, or non-equal intervals like Chebyshev–Gauss–Lobatto grid points, or with the normalization of the routes of Legendre polynomials'' (Shu, 2000). According to the results of previous researches, including the author's, the approaches proposed by Chebyshev-Gauss-Lobatto for grid points provided the most suitable node distributions in DQM. Therefore, in the present study, this approach is used as follows:

$$x_i = x_1 + \frac{1}{2}\left(1 - cos\frac{i-1}{N-1}\pi\right)(x_n - x_1) \qquad i = 1,2,\dots,N \tag{10}$$

And the derivative of the time for the first-order for point $i$ is substituted by the following relation:

$$\frac{\partial c_{1i}}{\partial t} = \frac{c_{1i}^t - c_{1i}^{t-\Delta t}}{\Delta t} \tag{11}$$

where $c_{1i}^t$ and $c_{1i}^{t-\Delta t}$ are the values at time level $t$ (new-time) and time level $t$-$\Delta t$ (old-time), respectively. By using this expression, Eq. (5) is re-written as follows:

$$R_1 \frac{c_{1i}^t - c_{1i}^{t-\Delta t}}{\Delta t} = D \sum_{j=1}^N b_{ij} C_{1j} - v \sum_{j=1}^N a_{ij} C_{1j} - k_1 C_{1i} \tag{12}$$

By selecting the values of the right-hand side of Eq. (12) as $t$, it means that the solution is calculated in fully implicit form. Thus, by employing some manipulations, the ultimate form of fully implicit solution is given as follows:

$$c_{1i}^t + \frac{\Delta t.v}{R_1}\sum_{j=1}^N a_{ij} C_1^t{}_j - \frac{\Delta t.D}{R_1}\sum_{j=1}^N b_{ij} C_1^t{}_j = c_{1i}^{t-\Delta t} - \frac{\Delta t k_1}{R_1} c_{1i}^{t-\Delta t} \tag{13}$$

And by using the following coefficients $Y_{i_1} = \frac{\Delta t.v}{R_1}$, $G_{i_1} = \frac{\Delta t.D}{R_1}$, and $K_1 = \frac{\Delta t k_1}{R_1}$ the matrix form of the solution is given as:

$$S = \begin{bmatrix} 1 + Y_{1_1}a_{11} - G_{1_1}b_{11} & Y_{1_1}a_{12} - G_{1_1}b_{12} & \dots & Y_{1_1}a_{1N} - G_{1_1}b_{1N} \\ Y_{2_1}a_{21} - G_{2_1}b_{21} & 1 + Y_{2_1}p_{22} - G_{2_1}b_{22} & \dots & Y_{2_1}a_{2N} - G_{2_1}b_{2N} \\ \vdots & \vdots & \ddots & \vdots \\ Y_{N_1}a_{N1} - G_{N_1}b_{N1} & Y_{N_1}a_{N2} - G_{N_1}b_{N2} & \dots & 1 + Y_{N_1}a_{NN} - G_{N_1}b_{NN} \end{bmatrix}$$

$$C = \begin{bmatrix} c_{11}^t \\ c_{12}^t \\ \vdots \\ c_{1N}^t \end{bmatrix} \qquad R = \begin{bmatrix} c_{11}^{t-\Delta t} - K_1 c_{11}^{t-1} \\ c_{12}^{t-\Delta t} - K_1 c_{12}^{t-1} \\ \vdots \\ c_{1N}^{t-\Delta t} - K_1 c_{1N}^{t-1} \end{bmatrix} \qquad \text{C.S=R} \tag{14}$$

It is worth noting that the solution process of both numerical methods applied here, should be solved in matrix form since the numerical models are provided in fully implicit form. By

enforcing the similar process for other species, the final forms of solution for the second-, third- and fourth-species are extracted as follows:

$$C_{2_i}^t + \frac{\Delta t.v}{R_2} \sum_{j=1}^N a_{ij} C_{2_j}^t - \frac{\Delta t.D}{R_2} \sum_{j=1}^N b_{ij} C_{2_j}^t = C_{2_i}^{t-\Delta t} - \frac{\Delta t k_2}{R_2} C_{2_i}^{t-\Delta t} + \frac{\Delta t k_1}{R_2} C_{1_i}^{t-\Delta t} \qquad (15)$$

$$C_{3_i}^t + \frac{\Delta t.v}{R_3} \sum_{j=1}^N a_{ij} C_{3_j}^t - \frac{\Delta t.D}{R_3} \sum_{j=1}^N b_{ij} C_{3_j}^t = C_{3_i}^{t-\Delta t} - \frac{\Delta t k_3}{R_3} C_{3_i}^{t-\Delta t} + \frac{\Delta t k_2}{R_3} C_{2_i}^{t-\Delta t} \qquad (16)$$

$$C_{4_i}^t + \frac{\Delta t.v}{R_4} \sum_{j=1}^N a_{ij} C_{4_j}^t - \frac{\Delta t.D}{R_4} \sum_{j=1}^N b_{ij} C_{4_j}^t = C_{4_i}^{t-\Delta t} - \frac{\Delta t k_4}{R_4} C_{4_i}^{t-\Delta t} + \frac{\Delta t k_3}{R_4} C_{3_i}^{t-\Delta t} \qquad (17)$$

As noted previously, to compare the outcomes of the suggested model with IDQM, the governing equations were solved with IFOFDM, too. In this step of the numerical experiment, to derive the appropriate form of the discretization, the relations for first- and second-order derivatives in time and spaces are written as follows (Kaya and Gharehbaghi, 2014):

$$\frac{\partial C_1}{\partial t} = \frac{c_{1_i}^t - c_{1_i}^{t-\Delta t}}{\Delta t} \qquad (18)$$

$$\frac{\partial C_1}{\partial x} = \frac{C_{1_{i-2}} - 8C_{1_{i-1}} + 8C_{1_{i+1}} - C_{1_{i+2}}}{12\Delta x} + o(\Delta x^4) \qquad (19)$$

$$\frac{\partial^2 C_1}{\partial x^2} = \frac{-C_{1_{i-2}} + 16C_{1_{i-1}} - 30C_{1_i} + 16C_{1_{i+1}} - C_{1_{i+2}}}{12\Delta x^2} + o(\Delta x^4) \qquad (20)$$

"The key idea of finite difference method relies on the conversation of continuous functions to their discretely sampled counterparts. To obtain these discrete sample points, the whole problem domain is decomposed into the regular grid" (Verma, and Wille (2021)). In this study, the equal interval node distribution approach for IFOFDM is used to determine grid points. By replacing Eq.'s (18–20) into Eq. (1), the solution of IFOFDM for the first-member is given as follows:

$$R_1 \frac{c_{1_i}^t - c_{1_i}^{t-\Delta t}}{\Delta t} = D \frac{-C_{1_{i-2}}^t + 16C_{1_{i-1}}^t - 30C_{1_i}^t + 16C_{1_{i+1}}^t - C_{1_{i+2}}^t}{12\Delta x^2} -$$

$$v \frac{C_{1_{i-2}}^t - 8C_{1_{i-1}}^t + 8C_{1_{i+1}}^t - C_{1_{i+2}}^t}{12\Delta x} - k_1 C_{1_i}^t \qquad (21)$$

And by some manipulation, the final form of the solution is obtained as:

$$C_{1_{i-2}}^t \left( \frac{\Delta t D}{12\Delta x^2 R_1} + \frac{\Delta t v}{12\Delta x R_1} \right) + C_{1_{i-1}}^t \left( -\frac{16\Delta t D}{12\Delta x^2 R_1} - \frac{8\Delta t v}{12\Delta x R_1} \right) + C_{1_i}^t \left( 1 + \frac{30\Delta t D}{12\Delta x^2 R_1} + \frac{\Delta t}{R_1} k_1 \right) +$$

$$C_{1_{i+1}}^t \left( -\frac{16\Delta t D}{12\Delta x^2 R_1} + \frac{8\Delta t v}{12\Delta x R_1} \right) + C_{1_{i+2}}^t \left( \frac{\Delta t D}{12\Delta x^2 R_1} - \frac{\Delta t v}{12\Delta x R_1} \right) = c_{1_i}^{t-\Delta t} \qquad (22)$$

To present the final form of the solution (i.e., Eq. 22) in a simpler form, $ka_m$ and $kb_m$ coefficients are used as follows:

$$ka_m = \frac{\Delta t D}{12 \Delta x^2 R_m} \qquad\qquad m = 1, \dots, M; \qquad\qquad (23)$$

$$kb_m = \frac{\Delta t v}{12 \Delta x R_m} \qquad\qquad m = 1, \dots, M; \qquad\qquad (24)$$

And by replacing these coefficients Eq. (22) can rearrange as follows:

$$C_{1_{i-2}}^t(ka_1 + kb_1) + C_{1_{i-1}}^t(-16ka_1 - 8kb_1) + C_{1_i}^t\left(1 + 30ka_1 + \frac{\Delta t}{R_1}k_1\right) +$$
$$C_{1_{i+1}}^t(kb_1 + 8kb_1) + C_{1_{i+2}}^t(ka_1 - kb_1) = c_{1_i}^{t-\Delta t} \qquad\qquad (25)$$

By applying the same steps for other species, the last forms of solution of IFOFDM for second-, third- and fourth-species are written as follows:

$$C_{2_{i-2}}^t(ka_2 + kb_2) + C_{2_{i-1}}^t(-16ka_2 - 8kb_2) + C_{2_i}^t\left(1 + 30ka_2 + \frac{\Delta t k_2}{R_2}\right) +$$
$$C_{2_{i+1}}^t(-16ka_2 + 8kb_2) + C_{2_{i+2}}^t(ka_2 - kb_2) - \frac{\Delta t k_1}{R_2}C_{1_i}^t = C_{2_i}^{t-\Delta t} \qquad\qquad (26)$$

$$C_{3_{i-2}}^t(ka_3 + kb_3) + C_{3_{i-1}}^t(-16ka_3 - 8kb_3) + C_{3_i}^t\left(1 + \frac{30 \Delta t D}{12 \Delta x^2 R_3} + \frac{\Delta t k_3}{R_3}\right) +$$
$$C_{3_{i+1}}^t(-16ka_3 + 8kb_3) + C_{3_{i+2}}^t(ka_3 - kb_3) - \frac{\Delta t k_2}{R_3}C_{2_i}^t = C_{3_i}^{t-\Delta t} \qquad\qquad (27)$$

$$C_{4_{i-2}}^t(ka_4 + kb_4) + C_{4_{i-1}}^t(-16ka_4 - 8kb_4) + C_{4_i}^t\left(1 + \frac{30 \Delta t D}{12 \Delta x^2 R_4} + \frac{\Delta t k_4}{R_4}\right) +$$
$$C_{4_{i+1}}^t(-16ka_4 + 8kb_4) + C_{4_{i+2}}^t(ka_4 - kb_4) - \frac{\Delta t k_3}{R_4}C_{3_i}^t = C_{4_i}^{t-\Delta t} \qquad\qquad (28)$$

## 4. NUMERICAL EXPERIMENTS AND RESULTS

In this section, the analytical results of three well-established multi-species solute transport problems introduced by Pérez Guerrero et al., (2009) and Bauer et al., (2001) are employed to assess the accuracy and efficiency of the presented numerical model with IDQM. Furthermore, the outcomes of the suggested model are compared with the numerical results of the IFOFDM approach. The code of the proposed model has been generated in MATLAB.

In the first and second case studies, the analytical results of dimensionless concentration for a three-species nitrification chain ($NH_4^+ \rightarrow NO_2^- \rightarrow NO_3^-$) are employed. For the first case study, the length of the domain and duration were selected as 220cm and 200h, respectively. For benchmark purposes, in the second case study, the domain length and duration were applied as 110cm and 50h (much smaller time), respectively. The linear interpolation method has been used to access the required point values of reported analytical results.

Details of the problems for the first and second cases, including retardation coefficient ($R_m$), decay coefficient ($\lambda_m$), initial and boundary conditions, etc., are described in Table (1). It is worthwhile to mention that in tables and figures below, the first and second case studies are referred to as the analytical results of dimensionless concentration for the three-species nitrification chain ($NH_4^+ \rightarrow NO_2^- \rightarrow NO_3^-$) introduced by Pérez Guerrero et al., (2009) for 220cm, 200h, and 110cm, 50h, respectively, and case three is referred to the analytical results of four-member decay chain solute transport problems introduced by Bauer et al., (2001). Meanwhile, in all of the figures and tables below, the x, c, curve_1, curve_2, and curve_3 are the abbreviations of distance (cm), concentration (mM), results of analytical expressions introduced by Pérez Guerrero et al., (2009), for $NH_4^+$, $NO_2^-$, and $NO_3^-$, respectively. Moreover, IFOFDM_C1, IFOFDM_C2, IFOFDM_C3 are the abbreviations of numerical results of the developed model with IFOFDM (i.e., calculated dimensionless concentration) for $NH_4^+$, $NO_2^-$, and $NO_3^-$, respectively, and IDQM_C1, IDQM_C2, and IDQM_C3 are the abbreviations of numerical results of the developed model with IDQM (i.e., calculated dimensionless concentration) for $NH_4^+$, $NO_2^-$, and $NO_3^-$, respectively.

*Table 1 - Parameter values for the nitrification chain problem*

| Description | $NH_4^+$ (m=1) | $NO_2^-$ (m=2) | $NO_3^-$ (m=3) |
|---|---|---|---|
| Retardation coefficient ($R_m$) | 2 | 1 | 1 |
| Decay coefficient, $\lambda_m$ | 0 | 0.1 | 0 |
| First case→$C(x,1)$ | 0 | 0 | 0 |
| First case→$C(1,t)$ | 0.9982064510 | 0.001731801827 | 0.00006174718691 |
| First case→$C(N,t)$ | 1.199389159E-89 | 1.255589051E-12 | 0.0002545665546 |
| Second case→$C(x,1)$ | 0 | 0 | 0 |
| Second case→$C(1,t)$ | 0.9982064510 | 0.001731801827 | 0.00006174718691 |
| Second case→$C(N,t)$ | 5.1438380E-177 | 1.622019705E-50 | 2.260630087E-48 |
| Pore velocity=1 cmh$^{-1}$ | Dispersion | coefficient | D=0.18cm$^2$h$^{-1}$ |

The results of numerical experiments for the first and second test cases are summarized in figures (1) and (2) and Tables (2-4). These cases are solved with two different space and time intervals. The first case is solved with ($N_x$=221, $N_t$=5001) and ($N_x$=441, $N_t$= 8001) number of nodes in space ($N_x$) and time ($N_t$), and the second case is employed ($N_x$=221, $N_t$=1001) and ($N_x$=331, $N_t$=5001) numbers of nodes in space ($N_x$) and time ($N_t$) to run the calculation. The numerical outcomes of the first case in domain length and at the duration equal to 200h for all the nitrogen species are illustrated in figure (1). Similarly, the numerical results of the second case in domain length and at the duration equal to 50h for all the nitrogen species are demonstrated in figure (2). It is crucial to remember that the Chebyshev-Gauss-Lobatto formula provides a non-uniform distribution of nodes. Hence, it is pointless to talk about the distance between adjacent nodes. Consequently, in distance sections of the tables below regarding the DQM and IDQM approximations, Δx has been replaced with (..). According to the numerical results provided in the figures, it is evident that both the IDQM and IFOFDM are gained very close results to the analytical results. For this reason, to make a better

evaluation result, the total mean square error (TMSE), $L_2$- and $L_\infty$-norms are determined by the following relations. The results of the comparisons are given in Tables (2-4).

$$TMSE = \frac{\Sigma(c_{Numerical\ solution} - c_{analytical\ results})^2}{N} \tag{29}$$

$$||x||_2 = \sqrt{x_1^2 + x_2^2 + \cdots + x_{N-1}^2 + x_N^2} \tag{30}$$

$$||x||_\infty = max[|x_1|, |x_2|, \ldots, |x_N|] \tag{31}$$

"Although only radioactive decay is a true first-order process, also chemical and biological transformations can be often described approximately in terms of first-order decay"; Bauer et al., (2001). Consequently, the numerical solutions for convey of a decay chain in porous media are widely applicable. According to the outcomes presented in the tables below, it can be revealed that both IDQM and IFOFDM approaches can estimate reliable outcomes and show good agreements with the results of analytical values. Based on the table of TMSE, in both first- and second-case studies, in the first- ($NH_4^+$) and third-members ($NO_3^-$) the numerical results of the IDQM are slightly better and in the second-member ($NO_2^-$), the IFOFDM have calculated slightly better results than IDQM. Nevertheless, by considering the numerical outcomes of $L_2$- and $L_\infty$-norms are given in tables 3 and 4, in the first-member ($NH_4^+$) the numerical results of the IDQM are slightly better, and in the second- ($NO_2^-$) and third- member ($NO_3^-$) the IFOFDM has computed slightly better results than IDQM. Moreover, with regard to the execution time, IDQM is required more execution time to obtain the outcomes than IFOFDM. These two test cases conclude that although numerical results of both of the methods are close to each other the results of IDQM are more reliable.
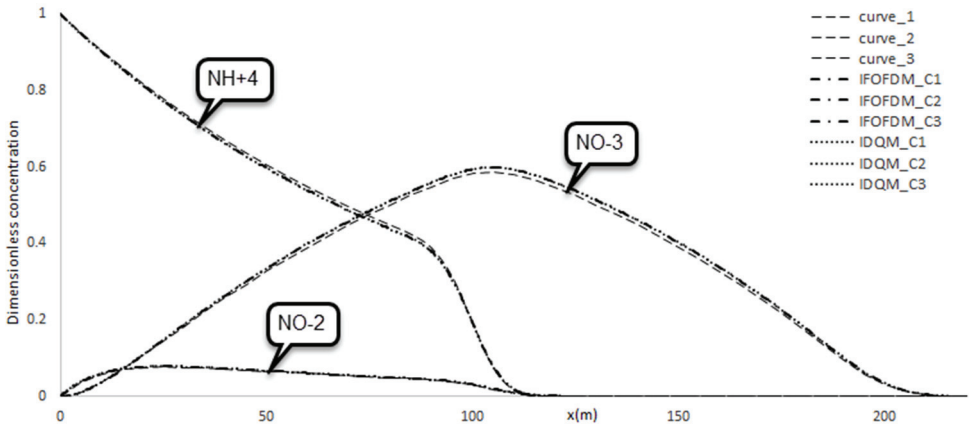


*Fig. 1 - Illustration of results of first case for 1D transient concentration distribution for all the nitrogen species (220cm and 200h) and ($N_x$=441, $N_t$=8001).*
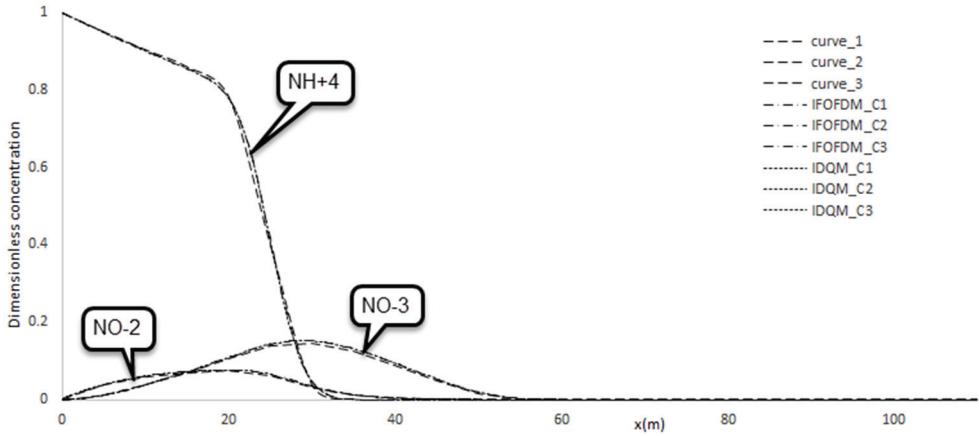
*Fig. 2 - Illustration of results of second case for 1D transient concentration distribution for all the nitrogen species (110cm and 50h) and ($N_x$=221, $N_t$=1001).*

*Table 2 - Table of TMSE for the first and second cases*

| Description | Nx(Δx); Nt(Δt) | $NH_4^+$ (m=1) | $NO_2^-$ (m=2) | $NO_3^-$ (m=3) | Execution time(s) |
|---|---|---|---|---|---|
| First case→IDQM | 221(..);5001(0.04) | 2.23187E-05 | 1.5288E-06 | 5.72399E-05 | 126.378909 |
| First case→IFOFDM | 221(1);5001(0.04) | 2.43501E-05 | 9.72845E-07 | 8.08827E-05 | 61.511134 |
| First case→IDQM | 441(..);8001(0.025) | 2.22319E-05 | 1.53588E-06 | 5.68567E-05 | 851.121429 |
| First case→IFOFDM | 441(0.5);8001(0.025) | 2.68109E-05 | 1.05194E-06 | 8.05886E-05 | 371.228101 |
| Second case→IDQM | 221(..);1001(0.05) | 9.15407E-05 | 2.51205E-06 | 8.01173E-06 | 31.272120 |
| Second case→IFOFDM | 221(0.5);1001(0.05) | 0.000124512 | 2.31983E-06 | 1.07669E-05 | 17.430015 |
| Second case→IDQM | 331(..);5001(0.01) | 0.000111603 | 2.58196E-06 | 7.94743E-06 | 248.877210 |
| Second case→IFOFDM | 331(0.3333);5001(0.01) | 0.000148968 | 2.46452E-06 | 1.1026E-05 | 106.136469 |

*Table 3 - Table of L₂-norms for the first and second cases*

| L₂- | Description | Nx(Δx); Nt(Δt) | $NH_4^+$ (m=1) | $NO_2^-$ (m=2) | $NO_3^-$ (m=3) |
|---|---|---|---|---|---|
| | Values of analytical results for Chebyshev–Gauss–Lobatto node distribution | 221(..);5001(0.04) | 7.714794599 | 0.577455 | 4.441281364 |
| | IDQM | 221(..);5001(0.04) | 7.667190368 | 0.592854 | 4.55057 |
| | Values of analytical results for equal interval node distribution | 221(1);5001(0.04) | 6.570121269 | 0.607462 | 5.401541442 |
| | IFOFDM | 221(1);5001(0.04) | 6.514591873 | 0.62115 | 5.530701 |
| First case | Values of analytical results for Chebyshev–Gauss–Lobatto node distribution | 441(..);8001(0.025) | 10.88757454 | 0.816626 | 6.280916403 |
| | IDQM | 441(..);8001(0.025) | 10.82030731 | 0.838446 | 6.43531 |
| | Values of analytical results for equal interval node distribution | 441(0.5);8001(0.025) | 9.264546037 | 0.859011 | 7.638814144 |
| | IFOFDM | 441(0.5);8001(0.025) | 9.17891276 | 0.87859 | 7.822758 |

*Table 3 - Table of L₂-norms for the first and second cases (continue)*

| $L_2$- | Description | Nx($\Delta$x); Nt($\Delta$t) | $NH_4^+$ (m=1) | $NO_2^-$ (m=2) | $NO_3^-$ (m=3) |
|---|---|---|---|---|---|
| Second case | Values of analytical results for Chebyshev–Gauss–Lobatto node distribution | 221(..);1001(0.05) | 7.587391907 | 0.433717 | 0.788799473 |
| | IDQM | 221 (..);1001(0.05) | 7.601745166 | 0.455104 | 0.827535 |
| | Values of analytical results for equal interval node distribution | 221 (0.5);1001(0.05) | 6.104308005 | 0.449497 | 0.912087457 |
| | IFOFDM | 221 (0.5);1001(0.05) | 6.140133425 | 0.470554 | 0.957084 |
| | Values of analytical results for Chebyshev–Gauss–Lobatto node distribution | 331(..);5001(0.01) | 9.279202108 | 0.531191 | 0.966017155 |
| | IDQM | 331(..);5001(0.01) | 9.300437483 | 0.557605 | 1.01355 |
| | Values of analytical results for equal interval node distribution | 331(0.3333);5001(0.01) | 7.459270646 | 0.550474 | 1.117018559 |
| | IFOFDM | 331(0.3333);5001(0.01) | 7.50537397 | 0.576871 | 1.173536 |

*Table 4 - Table of L∞-norms for the first and second cases*

| $L_\infty$- | Description | Nx($\Delta$x); Nt($\Delta$t) | $NH_4^+$ (m=1) | $NO_2^-$ (m=2) | $NO_3^-$ (m=3) |
|---|---|---|---|---|---|
| First case | Values of analytical results for Chebyshev–Gauss–Lobatto node distribution | 221(..);5001(0.04) | 0.998097 | 0.07701 | 0.586774641 |
| | IDQM | 221(..);5001(0.04) | 0.998091 | 0.079031 | 0.598597 |
| | Values of analytical results for equal interval node distribution | 221(1);5001(0.04) | 0.988487 | 0.077057 | 0.587139464 |
| | IFOFDM | 221(1);5001(0.04) | 0.989172 | 0.079023 | 0.598491 |
| | Values of analytical results for Chebyshev–Gauss–Lobatto node distribution | 441(..);8001(0.025) | 0.998179 | 0.077017 | 0.586774641 |
| | IDQM | 441(..);8001(0.025) | 0.998178 | 0.079036 | 0.598795 |
| | Values of analytical results for equal interval node distribution | 441(0.5);8001(0.025) | 0.993347 | 0.077057 | 0.587139464 |
| | IFOFDM | 441(0.5);8001(0.025) | 0.993638 | 0.079035 | 0.598705 |
| Second case | Values of analytical results for Chebyshev–Gauss–Lobatto node distribution | 221(..);1001(0.05) | 0.998152 | 0.074356 | 0.14623526 |
| | IDQM | 221 (..);1001(0.05) | 0.998149 | 0.076721 | 0.152878 |
| | Values of analytical results for equal interval node distribution | 221 (0.5);1001(0.05) | 0.993347 | 0.074712 | 0.146364487 |
| | IFOFDM | 221 (0.5);1001(0.05) | 0.993638 | 0.076723 | 0.152725 |
| | Values of analytical results for Chebyshev–Gauss–Lobatto node distribution | 331(..);5001(0.01) | 0.998182 | 0.074526 | 0.146065318 |
| | IDQM | 331(..);5001(0.01) | 0.998180849 | 0.076808 | 0.153172 |
| | Values of analytical results for equal interval node distribution | 331(0.3333);5001(0.01) | 0.994967 | 0.074712 | 0.146364487 |
| | IFOFDM | 331(0.3333);5001(0.01) | 0.995139634 | 0.076811 | 0.153123 |

The third case study is used an arbitrary decay chain with four species in an arbitrary complex porosity medium in the 3000 m and 3000 days. The implementation of these domain lengths and durations shows that the developed model can solve semi-infinite and long-term problems. The details of the problem for the third case study are presented in Table (5). Besides, in all of the figures and tables below related to the third case, the x, c, C1, C2, C3, C4, IDQM_C1, IDQM _C2, IDQM _C3, IDQM _C4, IFOFDM_C1, IFOFDM_C2, IFOFDM_C3, and IFOFDM_C4 are the abbreviations of distance (cm), concentration (mM), outcomes of analytical expressions for the concentration introduced by Bauer et al., (2001) for four species, numerical results of the concentration with the suggested model for IDQM for four species, and numerical results of the concentration with the suggested model for IFOFDM for four species, respectively. This case study is solved for six different space and time intervals, including $N_x=101$, $N_t=3001$; $N_x=101$, $N_t=10001$; $N_x=301$, $N_t=3001$; $N_x=301$, $N_t=10001$; Nx=501, $N_t=1501$; and Nx=501, $N_t=10001$. Similar to the two earlier cases to make a better evaluation result, the TMSE, $L_2$- and $L_\infty$-norms are determined, too. The outcomes of the comparisons have given in Tables (6-8). The numerical results of concentration distributions for the four-member decay chain for this case study for $N_x=501$, $N_t=1501$ are presented in figure (3). The numerical results presented in Tables (6-8) show that for all of the implemented space and time intervals, the numerical results of the IDQM are more accurate than the IFOFDM. But according to the values given in the tables below, with fewer numbers of space and time node points, the IDQM has obtained more reliable results than IFOFDM. Furthermore, based on these results, the IDQM requires more execution time than IFOFDM.
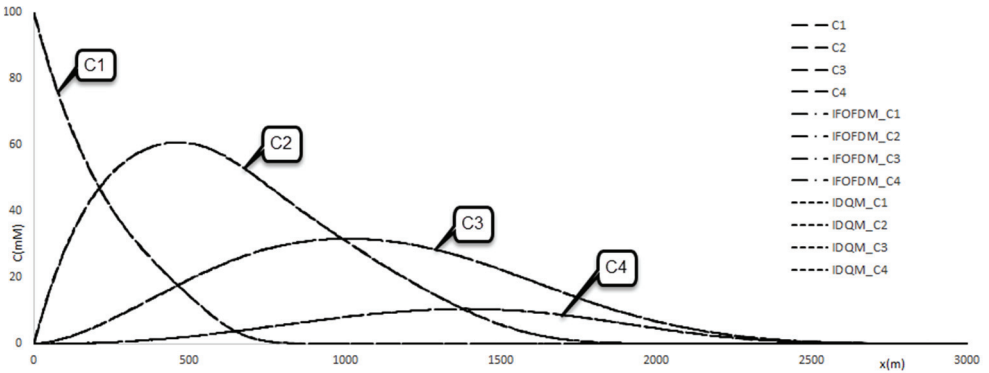


*Fig. 3 - 1D transient concentration distribution for constant boundary condition (3000m and 3000day) in (Nx=501, Nt=1501).*

*Table 5 - Parameter values for the third case*

| Description | $C_1$ (m=1) | $C_2$ (m=2) | $C_3$ (m=3) | $C_4$ (m=4) |
|---|---|---|---|---|
| Retardation coefficient ($R_m$) | 5.3 | 1.9 | 1.2 | 1.3 |
| Decay coefficient, $\lambda_m \times 10^{-4}$ (day$^{-1}$) | 7 | 5 | 4.5 | 3.8 |
| Third case→$C(x,1)$ (mM) | 0 | 0 | 0 | 0 |
| Third case →$C(1,t)$ (mM) | 100 | 0 | 0 | 0 |
| Third case→$C(N,t)$ (mM) | 0 | 0 | 0 | 0 |
| Pore velocity=1 mday$^{-1}$ | Dispersoin | coefficient | D=10m$^2$day$^{-1}$ | |

*Table 6 - Table of TMSE for the third case*

| Description | Nx(Δx); Nt(Δt) | C₁ (m=1) | C₂ (m=2) | C₃ (m=3) | C₄ (m=4) | Execution time(s) |
|---|---|---|---|---|---|---|
| Third case→IDQM | 101(..);3001(1) | 0.02303187 | 0.015139854 | 0.001525551 | 0.001407 | 66.787963 |
| Third ase→IFOFDM | 101(30);3001(1) | 0.106788638 | 0.104846677 | 0.010803551 | 0.00228 | 12.547559 |
| Third case→IDQM | 101(..);10001(0.3) | 0.027600203 | 0.014447211 | 0.001497311 | 0.001468 | 110.461599 |
| Third ase→IFOFDM | 101(30);10001(0.3) | 0.10734477 | 0.106451881 | 0.0103502 | 0.002098 | 38.984924 |
| Third case→IDQM | 301(..);3001(1) | 0.02303187 | 0.015139854 | 0.001525551 | 0.001407 | 190.529084 |
| Third ase→IFOFDM | 301(10);3001(1) | 0.013655793 | 0.01813048 | 0.002349908 | 0.001684 | 66.787963 |
| Third case→IDQM | 301(..);10001(0.3) | 0.023034354 | 0.01507317 | 0.001487377 | 0.001532 | 560.674821 |
| Third ase→IFOFDM | 301(10);10001(0.3) | 0.01373847 | 0.018717975 | 0.002112538 | 0.001659 | 187.716471 |
| Third case→IDQM | 501(..);1501(2) | 0.023435438 | 0.015701183 | 0.002425594 | 0.001617 | 221.940376 |
| Third ase→IFOFDM | 501(6);1501(2) | 0.007617517 | 0.009957415 | 0.002738082 | 0.001915 | 97.215048 |
| Third case→IDQM | 501(..);10001(0.3) | 0.023374174 | 0.015127306 | 0.001491743 | 0.001537 | 1561.336216 |
| Third ase→IFOFDM | 501(6);10001(0.3) | 0.007640485 | 0.010622715 | 0.001749389 | 0.001684 | 641.655791 |

*Table 7 - Table of L₂-norms for the third case*

| L₂- | Description | Nx(Δx); Nt(Δt) | C₁ (m=1) | C₂ (m=2) | C₃ (m=3) | C₄ (m=4) |
|---|---|---|---|---|---|---|
| | Values of analytical results for Chebyshev–Gauss–Lobatto node distribution | 101(..);3001(1) | 355.846 | 273.52 | 149.7069 | 46.23924 |
| | IDQM | 101(..);3001(1) | 356.8835 | 273.4465 | 149.6668 | 46.1735 |
| | Values of analytical results for equal interval node distribution | 101(30);10001(1) | 224.8856 | 287.7221 | 179.0449 | 56.97991 |
| | IFOFDM | 101(30);10001(1) | 227.6443 | 287.4638 | 178.8244 | 56.80733 |
| Third case | Values of analytical results for Chebyshev–Gauss–Lobatto node distribution | 101(..);10001(0.3) | 355.846 | 273.52 | 149.7069 | 46.23924 |
| | IDQM | 101(..);10001(0.3) | 356.8847 | 273.4378 | 149.6295 | 46.14533 |
| | Values of analytical results for equal interval node distribution | 101(30);10001(0.3) | 224.8856 | 287.7221 | 179.0449 | 56.97991 |
| | IFOFDM | 101(30);10001(0.3) | 227.6506 | 287.5197 | 178.8753 | 56.82232 |
| | Values of analytical results for Chebyshev–Gauss–Lobatto node distribution | 301(..);3001(1) | 608.5267 | 473.7572 | 259.2994 | 80.10468 |
| | IDQM | 301(..);3001(1) | 609.9979 | 473.6232 | 259.2306 | 79.97485 |
| | Values of analytical results for equal interval node distribution | 301(10);3001(1) | 375.774 | 498.2827 | 310.115 | 98.69671 |
| | IFOFDM | 301(10);3001(1) | 377.5027 | 498.1249 | 309.7794 | 98.40844 |
| | Values of analytical results for Chebyshev–Gauss–Lobatto node distribution | 301(..);10001(0.3) | 608.5267 | 473.7572 | 259.2994 | 80.10468 |
| | IDQM | 301(..);10001(0.3) | 610 | 473.6082 | 259.1658 | 79.92606 |
| | Values of analytical results for equal interval node distribution | 301(10);10001(0.3) | 375.774 | 498.2827 | 310.115 | 98.69671 |
| | IFOFDM | 301(10);10001(0.3) | 377.5141 | 498.2218 | 309.8675 | 98.43445 |
| | Values of analytical results for Chebyshev–Gauss–Lobatto node distribution | 501(..);1501(2) | 783.485 | 611.647 | 334.7578 | 103.4202 |

*Table 7 - Table of L₂-norms for the third case (continue)*

| L₂- | Description | Nx(Δx); Nt(Δt) | C₁ (m=1) | C₂ (m=2) | C₃ (m=3) | C₄ (m=4) |
|---|---|---|---|---|---|---|
| | IDQM | 501(..);1501(2) | 785.3808 | 611.4726 | 334.785 | 103.3376 |
| | Values of analytical results for equal interval node distribution | 501(6);1501(2) | 481.6137 | 643.2655 | 400.3579 | 127.4187 |
| | IFOFDM | 501(6);1501(2) | 483.0585 | 642.916 | 399.7652 | 126.9986 |
| | Values of analytical results for Chebyshev–Gauss–Lobatto node distribution | 501(..);10001(0.3) | 783.485 | 611.647 | 334.7578 | 103.4202 |
| | IDQM | 501(..);10001(0.3) | 785.3874 | 611.4256 | 334.5817 | 103.1841 |
| | Values of analytical results for equal interval node distribution | 501(6);10001(0.3) | 481.6137 | 643.2655 | 400.3579 | 127.4187 |
| | IFOFDM | 501(6);10001(0.3) | 483.0947 | 643.2195 | 400.041 | 127.0796 |

*Table 8 - Table of L∞-norms for the third case*

| L∞- | Description | Nx(Δx); Nt(Δt) | C₁ (m=1) | C₂ (m=2) | C₃ (m=3) | C₄ (m=4) |
|---|---|---|---|---|---|---|
| | Values of analytical results for Chebyshev–Gauss–Lobatto node distribution | 101(..);3001(1) | 98.72462 | 60.67081 | 31.68947 | 10.47882 |
| | IDQM | 101(..);3001(1) | 99.7352472 | 60.7669 | 31.66417 | 10.43484 |
| | Values of analytical results for equal interval node distribution | 101(30);10001(1) | 89.75127 | 60.70631 | 31.69296 | 10.48347 |
| | IFOFDM | 101(30);10001(1) | 90.9395646 | 60.72168 | 31.64842 | 10.42173 |
| Third case | Values of analytical results for Chebyshev–Gauss–Lobatto node distribution | 101(..);10001(0.3) | 98.72462 | 60.67081 | 31.68947 | 10.47882 |
| | IDQM | 101(..);10001(0.3) | 99.7352472 | 60.77122 | 31.664 | 10.43486 |
| | Values of analytical results for equal interval node distribution | 101(30);10001(0.3) | 89.75127 | 60.70631 | 31.69296 | 10.48347 |
| | IFOFDM | 101(30);10001(0.3) | 90.9395646 | 60.72967 | 31.66032 | 10.42911 |
| | Values of analytical results for Chebyshev–Gauss–Lobatto node distribution | 301(..);3001(1) | 99.7783 | 60.75209 | 31.69223 | 10.485 |
| | IDQM | 301(..);3001(1) | 99.9705462 | 60.78502 | 31.67563 | 10.43887 |
| | Values of analytical results for equal interval node distribution | 301(10);3001(1) | 96.30834 | 60.76353 | 31.69298 | 10.485 |
| | IFOFDM | 301(10);3001(1) | 96.8136065 | 60.77551 | 31.65793 | 10.42804 |
| | Values of analytical results for Chebyshev–Gauss–Lobatto node distribution | 301(..);10001(0.3) | 99.7783 | 60.75209 | 31.69223 | 10.485 |
| | IDQM | 301(..);10001(0.3) | 99.97055 | 60.78889 | 31.67536 | 10.43902 |
| | Values of analytical results for equal interval node distribution | 301(10);10001(0.3) | 375.774 | 498.2827 | 310.115 | 98.69671 |
| | IFOFDM | 301(10);10001(0.3) | 377.5141 | 498.2218 | 309.8675 | 98.43445 |
| | Values of analytical results for Chebyshev–Gauss–Lobatto node distribution | 501(..);1501(2) | 99.92019 | 60.76635 | 31.70456 | 10.485 |
| | IDQM | 501(..);1501(2) | 99.9894 | 60.778 | 31.676 | 10.43835 |
| | Values of analytical results for equal interval node distribution | 501(6);1501(2) | 97.53872 | 60.78184 | 31.69583 | 10.485 |

*Table 8 - Table of L∞-norms for the third case (continue)*

| $L_\infty$- | Description | Nx($\Delta$x); Nt($\Delta$t) | $C_1$ (m=1) | $C_2$ (m=2) | $C_3$ (m=3) | $C_4$ (m=4) |
|---|---|---|---|---|---|---|
| | IFOFDM | 501(6);1501(2) | 98.0604 | 60.77047 | 31.64168 | 10.41751 |
| | Values of analytical results for Chebyshev–Gauss–Lobatto node distribution | 501(..);10001(0.3) | 99.92019 | 60.76635 | 31.70456 | 10.485 |
| | IDQM | 501(..);10001(0.3) | 99.9894 | 60.78784013 | 31.6753 | 10.43872 |
| | Values of analytical results for equal interval node distribution | 501(6);10001(0.3) | 97.53872 | 60.78184 | 31.69583 | 10.485 |
| | IFOFDM | 501(6);10001(0.3) | 98.0603959 | 60.78666 | 31.67011 | 10.43577 |

## 5. CONCLUSION

In the present study, for the first time, a novel numerical model for multi-species solute transport phenomenon based on the IDQM is established and effectively analysed. Furthermore, the IFOFDM is used to compare the performance of the suggested model. Although there is no restriction in the number of multi-species, the analytical results of three different three-species ($NH_4^+ \rightarrow NO_2^- \rightarrow NO_3^-$) and four-species problems reported in the literature are employed for numerical interpretation of the developed model. Presented results proved that both numerical models with IDQM and IFOFDM for each species converged to previously reported literature values, and a good agreement is found between both the numerical solutions for all of the three-species and four-species problems. TMSE, $L_2$- and $L_\infty$-norms have been applied for in-depth evaluation of numerical results. All case studies were simulated with at least two different space and time intervals. In all cases, the numerical results of IDQM are better than the numerical results of IFOFDM. In the first two case studies, the numerical results of IDQM for the ($NH_4^+$) and ($NO_3^-$) members are more accurate. In the last case study based on the numerical results of six numerical experiments, it is obviously clear that the numerical outcomes of the IDQM are more accurate and reliable than the IFOFDM. The third case study demonstrated that the established model is able to predict long-term problems in the semi-infinite domain. Moreover, despite the high accuracy, the application of the IDQM needs less computational effort compared to other implemented numerical methods, and the application process is not complicated. In addition, low memory storage requirement is another advantage of this method. The only weak point of the IDQM is related to the execution time for integration, which increases due to the structure of the coefficient matrix. Consequently, it can be stated that although the IDQM provides better results, by considering the execution time may be IFOFDM is more economical to use.

## Acknowledgements

## References

[1]  Bagalkot, N., Kumar, G.S., 2015. Effect of nonlinear sorption on multispecies radionuclide transport in a coupled fracture-matrix system with variable fracture aperture: a numerical study. ISH Journal of Hydraulic Engineering. 21(3) 242–254, http://dx.doi.org/10.1080/09715010.2015.1016125

[2]  Bauer, P., Attinger, S., Kinzelbach, W., 2001. Transport of a decay chain in homogenous porous media: analytical solutions, Journal of Contaminant Hydrology. 49, 217–239.

[3]  Bellman, R., Casti, J., 1971. Differential quadrature and long-term integration. J. Math. Anal. Appl. 34 (2), 235–238.

[4]  Chaudhary, M., Singh, M.K. 2020, Study of multispecies convection-dispersion transport equation with variable parameters, Journal of Hydrology 591 (2020), https://doi.org/10.1016/j.jhydrol.2020.125562

[5]  Chen, W. and Zhong, T., 1997, The study on the nonlinear computations of the DQ and DC methods. Numerical Methods for Partial Differential Equations, 13, 57–75

[6]  Chen-Charpentier, B.M., Dimitrov, D.T., Kojouharov H.V., 2009. Numerical simulation of multi-species biofilms in porous media for different kinetics, Mathematics and Computers in Simulation, 79, 1846–1861.

[7]  Ciftci, E., 2017. Modelling coupled density-dependent flow and solute transport with the differential quadrature method, Geosciences Journal, 21(5), 807−817, http://dx.doi.org/10.1007/s12303-017-0009-5

[8]  Konikow, L.F., and Bredehoeft, J.D., 1978, Computer model of two-dimensional solute transport and dispersion in ground water: U.S. Geological Survey, Techniques of Water-Resources Investigations, Book 7, Chap. C2.

[9]  Civalek, O. 2004, Application of differential quadrature (DQ) and harmonic differential quadrature (HDQ) for buckling analysis of thin isotropic plates and elastic columns, Engineering Structures, 26,171–186.

[10]  Das, P., Akhter, A., Singh, M.K., 2018. Solute transport modelling with the variable temporally dependent boundary, Sadhana, 43, 1-12, https://doi.org/10.1007/s12046-017-0778-6

[11]  Essaid, H.I. and Bekins, B.A., 1997, BIOMOC, A Multispecies Solute-Transport Model with Biodegradation, U.S. GEOLOGICAL SURVEY, Water-Resources Investigations Report 97-4022.

[12]  Gharehbaghi, A., 2016. Explicit and implicit forms of differential quadrature method for advection–diffusion equation with variable coeffcients in semi-infnite domain, J. Hydrol. 541 (1), 935–940, http://dx.doi.org/10.1016/j.jhydrol.2016.08.002

[13]  Gharehbaghi, A., 2017. Third- and fifth-order finite volume schemes for advection–diffusion equation with variable coefficients in semi-infinite domain. Water and Environment Journal. 31 (2), 184–193. doi:10.1111/wej.12233

[14] Gharehbaghi, A., Kaya, B., Saadatnejadgharahassanlou, H., 2017. Two-dimensional bed variation models under nonequilibrium conditions in turbulent streams. Arabian Journal for Science and Engineering. 42 (3), 999–1011.

[15] Kaya, B., 2010. Solution of the advection-diffusion equation using the differential quadrature method. KSCE J. Civil Eng. 14 (1), 69–75.

[16] Kaya, B., Arisoy, Y., 2011. Differential quadrature solution for one-dimensional aquifer flow, Mathematical and Computational Applications, 16(2), 524-534.

[17] Kaya, B., Gharehbaghi., A., 2014. Implicit Solutions of Advection Diffusion Equation by Various Numerical Methods. Aust. J. Basic & Appl. Sci., 8(1): 381-391.

[18] Kumar, A., Kumar, D., Kumar, J.N., 2010. Analytical solutions to one-dimensional advection–diffusion equation with variable coefficients in semi-infinite media. J. Hydrol. 380, 330–337.

[19] Massoudieh, A., Ginn, T.R., 2007, Modeling colloid-facilitated transport of multi-species contaminants in unsaturated porous media, Journal of Contaminant Hydrology 92, 162–183, doi:10.1016/j.jconhyd.2007.01.005

[20] Engdahl N.B., Aquino, T., 2018, Considering the utility of backward-in-time simulations of multi-component reactive transport in porous media, Advances in Water Resources, 119, 17–27. https://doi.org/10.1016/j.advwatres.2018.06.003

[21] Natarajan N., Kumar S.G., 2010. Finite difference approach for modeling multispecies transport in porous media, International Journal of Engineering Science and Technology. 2(8), 3344-3350.

[22] Pathania, T., Eldho, T.I., Bottacin-Busolin, A. 2020. Coupled simulation of groundwater flow and multispecies reactive transport in an unconfined aquifer using the element-free Galerkin method. Engineering Analysis with Boundary Elements. 121, 31–49.

[23] Pérez Guerrero, J.S., Skaggs, T.H., van Genuchten, M.Th., 2009. Analytical Solution for Multi-Species Contaminant Transport Subject to Sequential First-Order Decay Reactions in Finite Media. Transp Porous Med. 80, 373–387, DOI 10.1007/s11242-009-9368-3

[24] Ramos, T.B., Šimůnek, J., Gonçalves, M.C., Martins, J.C., Prazeres, A., Castanheira, N.L., Pereira, L.S., 2011, Field evaluation of a multicomponent solute transport model in soils irrigated with saline waters, Journal of Hydrology, 407(1–4), 129-144, https://doi.org/10.1016/j.jhydrol.2011.07.016.

[25] Savovic, S., Djordjevich, A., 2012. Finite difference solution of the one-dimensional advection–diffusion equation with variable coefficients in semi-infinite media. Int. J. Heat Mass Transf. 55, 4291–4294. http://dx.doi.org/10.1016/j.ijheatmasstransfer.2012.03.073

[26] Sharma A., Guleria, A., Swami D., 2016. Numerical modelling of multispecies solute transport in porous media. Hydro 2016 international conference. 159-169.

[27] Shu, C., 2000. Differential Quadrature and its Application in Engineering. first ed.Springer-Verlag, London Limited.

[28] Šimůnek, J., Šejna, M., Saito, H., Sakai, M., and van Genuchten, M. Th., 2012, The HYDRUS-1D Software Package for Simulating the One-Dimensional Movement of Water, Heat, and Multiple Solutes in Variably-Saturated Media, university of california riverside riverside, California

[29] Singh, M.K., Ahamad S., and Singh, V.P., 2012. Analytical Solution for One-Dimensional Solute Dispersion with Time-Dependent Source Concentration along Uniform Groundwater Flow in a Homogeneous Porous Formation. Journal of Engineering Mechanics. 138(8).

[30] Sun, Y., Petersen, J. N., Clement, T. P., and Skeen, R. S., 1999, Development of analytical solutions for multispecies transport with serial and parallel reactions, water resources research, 35(1), 185-190.

[31] Torlapati, J., 2013. Development and Application of One Dimensional Multi-component Reactive Transport Models. Phd dissertation, Auburn, Alabama, USA, May 4, 2013

[32] Van Genuchten, M.Th., 1985, Convective-dispersive transport of solutes involved in sequential first-order decay reactions, Computers & Geosciences, 11(2), 129-147, https://doi.org/10.1016/0098-3004(85)90003-2.

[33] Verma, K., Wille, R., High Performance Simulation for Industrial Paint Shop Applications, Springer Nature, 2021

[34] Zhang, Z., Zhang, J., Ju, Z. Zhu, M. 2018, A one-dimensional transport model for multi-component solute in saturated soil, Water Science and Engineering, 11(3), 236-242, https://doi.org/10.1016/j.wse.2018.09.007.

[35] Zong, Z., Zhang, Y., 2009. Advanced Differential Quadrature Methods, first ed. CRC Press, Taylor and Francis Group, New York.